BRILL

IAWA Journal 35 (3), 2014: 217–235

iawa

PIT MEMBRANES OF *EPHEDRA* RESEMBLE GYMNOSPERMS MORE THAN ANGIOSPERMS

Roland R. Dute[1,*], **Lauren A. Bowen**[1], **Sarah Schier**[1], **Alexa G. Vevon**[1], **Troy L. Best**[1], **Maria Auad**[3], **Thomas Elder**[2], **Pauline Bouche**[4,5] and **Steven Jansen**[4]

[1]Department of Biological Sciences, Auburn University, Life Sciences Building, Auburn, Alabama 36849-5407, U.S.A.
[2]USDA-Forest Service, Southern Research Station, 2500 Shreveport Highway, Pineville, Louisiana 71360, U.S.A.
[3]Department of Polymer and Fiber Engineering, Auburn University, Auburn, Alabama, U.S.A.
[4]Institute for Systematic Botany and Ecology, Ulm University, Albert-Einstein-Allee 11, D-89081, Ulm, Germany
[5]UMR BIOGECO, INRA, University of Bordeaux, Avenue des Facultés Bat. B2, 33405 Talence, France
*Corresponding author; e-mail: duterol@auburn.edu

ABSTRACT

Bordered pit pairs of *Ephedra* species were characterized using different types of microscopy. Pit membranes contained tori that did not stain for lignin. SEM and AFM views of the torus surface showed no plasmodesmatal openings, but branched, secondary plasmodesmata were occasionally noted using TEM in conjunction with ultrathin sections. The margo consisted of radial microfibrils as well as finer diameter tangential fibrils. The former formed fascicles of fibrils that merged into even thicker buttresses during the act of pit membrane aspiration. AFM showed a discontinuous layer of non-microfibrillar material on the surface of both torus and margo. It is hypothesized that this material is responsible for adhesion of the pit membrane to the surface of the pit border during the process of aspiration. Taken as a whole, intervascular pit membranes of *Ephedra* more closely resemble those of conifers than those of torus-bearing pit membranes of angiosperms.

Keywords: Atomic force microscopy, margo, plasmodesmata, scanning electron microscopy, torus, transmission electron microscopy.

INTRODUCTION

Ephedra is a genus of about 50 spp. (Price 1996) found in semiarid and arid environments in both Northern and Southern Hemispheres (Joshi & Khan 2005; discussion Carlquist 2012). Alkaloids of some species have been used for many years as stimulants and bronchodilating agents (Joshi & Khan 2005).

Ephedra is of anatomical interest in that, although generally classified as a gymnosperm, its xylem contains vessel members as well as tracheids. The same is true for the

Published by Koninklijke Brill NV, Leiden
DOI 10.1163/22941932-00000062

Table 1. Sources of *Ephedra* wood specimens examined in this study.

Specimens from each collection are located in the Auburn University Herbarium (AUA). All collections were made in the USA.

Taxon	Date of collection	Collector(s) number	Treatment(s)	Collection site
E. fasciculata A. Nels.	5 May 1957	Demaree 58976	2, 4, 6	Coconino Co., Arizona
E. torreyana Wats.	14 May 1957	Demaree 38892	2, 4, 6	Coconino Co., Arizona
E. trifurca Torr. *ex* S. Wats.	10 Aug 2009	Hansen 4290	2, 4, 6	Doña Ana Co., New Mexico
E. trifurca Torr. *ex* S. Wats	9 Aug 2009	Hansen 4191	2, 6	Cochise Co., Arizona
E. viridis Cov.	23 Jun 1980	Crampton 9732	2, 4, 6	Lyon Co., Nevada
E. torreyana Wats.	4 Aug 2012	Best s.n.	1, 3, 5, 7, 8	Lincoln Co., New Mexico
E. torreyana Wats.	9 Aug 2012	Best s.n.	1, 3, 5	Otero Co., New Mexico
E. trifurca Torr. *ex* S. Wats	5 Aug 2012	Best s.n.	1, 3, 5, 7, 8	Socorro Co., New Mexico
E. trifurca Torr. *ex* S. Wats	6 Aug 2012	Best s.n.	1, 3, 5	Cochise Co., Arizona
E. trifurca Torr. *ex* S. Wats	7 Aug 2012	Best s.n.	1, 3, 5, 7, 8	Luna Co., New Mexico
E. viridis Cov.	4 Aug 2012	Best s.n.	1, 3, 5, 7, 8	Lincoln Co., New Mexico

Treatments: 1 = LM; 2 = AFM herbarium; 3 = AFM preserved; 4 = SEM herbarium; 5 = SEM preserved; 6 = TEM herbarium; 7 = TEM preserved; 8 = SEM resin removal. All samples were eight years in age or less. No attempt was made to correlate the results with other, older samples.

related genera *Gnetum* and *Welwitschia* (Thompson 1912, 1918; Carlquist & Gowans 1995). This observation has led to much speculation that perforations in *Ephedra* and *Gnetum* had evolved from circular bordered pits of coniferous tracheids and were of independent origin from the perforations of angiosperms. Studies late in the 20th century supported combining angiosperms, Gnetales, Bennettitales and *Pentoxylon* into a group identified as the anthophytes (Frohlich & Chase 2007). The hypothesis of Gnetaleans being more closely associated with angiosperms than with gymnosperms was strengthened by the discovery of double fertilization in *Ephedra* (Friedman 1990). However, recent consensus is that Gnetaleans are more closely related to conifers (Frohlich & Chase 2007).

The torus-margo pit membrane is present in both the conifers (Pittermann *et al*. 2005; Dute *et al*. 2008) and *Ginkgo biloba* L. (Dute 1994). *Ephedra* is also known to possess intervascular pit membranes with a torus-margo structure (Thompson 1912). Some species of *Gnetum* have tori of variable development, whereas in other spe-

cies the intervascular pit membranes are homogeneous (Carlquist 1994; Carlquist & Robinson 1995; Carlquist 1996). *Welwitschia mirabilis* Hook. seems to have homogeneous pit membranes, but there is a weak tendency to have a central thickening of the pit membrane, which looks torus-like (Jansen, pers. obs.). Carlquist (2012) also noticed at least one or two pit membranes in *Welwitschia* with an indistinct torus, but Carlquist and Gowans (1995) suggested that tori are absent in this genus.

Most species of angiosperms have intervascular pit membranes that are homogeneous, but some species do have the torus-margo construction (Dute *et al*. 2010). This laboratory has studied ontogeny of torus-bearing pit membranes for a number of years. Among some angiosperms, tori are deposited late in bordered pit development as pads on the surface of the compound middle lamella. The torus pads can be viewed basically as secondary wall deposits. Such a developmental mechanism has been assigned to *Osmanthus* (Dute & Rushing 1988), *Daphne* (Dute *et al*. 1990) and *Cercocarpus* (Dute *et al*. 2010). In contrast, tori in pit membranes of the genera *Celtis* and *Ulmus* (Dute & Rushing 1990) develop early (prior to pit border initiation) and represent thickening of the respective primary walls.

The present study uses different forms of microscopy, including atomic force microscopy (AFM), to characterize intervascular pit membranes of tracheary elements of *Ephedra*. No attempt is made in this study to distinguish features of pit membranes of vessel to tracheid contacts *versus* tracheid to tracheid contacts. Emphasis is placed on whether the pit membranes show features typical of angiosperms or gymnosperms.

MATERIALS AND METHODS

All specimens used in this study were taken from aerial stems.

Light microscopy

Field specimens were collected by Dr. Troy Best of Auburn University during August of 2012 (Table 1). Portions of each specimen were placed in FAA (formalin-acetic acid-alcohol) preservative (Johansen 1940). The remainder of each specimen was pressed for eventual inclusion in the Auburn University Herbarium (AUA). Three species were identified from among the specimens: *Ephedra torreyana* S. Watson, *E. trifurca* Torr. *ex* S. Watson and *E. viridis* Coville. Preserved tissue cubes of each species were dehydrated in an alcohol series (50% through 95%) and embedded in JB-4 plastic resin. Three micrometer-thick sections were cut with a Sorvall MT-2b ultramicrotome, heat-fixed to glass slides, and stained with either toluidine blue O (TBO, Ruzin 1999) or with $KMnO_4$ (Donaldson 2002) for 10 and 2 minutes, respectively (Dute *et al*. 2012). Stained sections were viewed and photographed with either a Nikon Biophot microscope with a NIKON D-70 digital camera or with a Nikon Eclipse 80i epifluorescence microscope (using brightfield setting) with a Qimaging Fast 1394 digital camera.

SEM

Herbarium samples – Air-dried wood samples taken from herbarium specimens (Table 1) were split longitudinally and attached to aluminum stubs (Electron Micros-

copy Sciences) using carbon-impregnated, double stick tape. Specimens were coated with gold-palladium and viewed with a Zeiss EVO 50 at 10–25 kV.

FAA samples – FAA-treated specimens were dehydrated through absolute ethanol and placed into two changes of hexamethyldisilazane (HMDS) for 18 h (Nation 1983). The samples were allowed to air-dry, mounted on aluminum SEM stubs, and sputter coated with gold (Electron Microscopy Sciences 550X) for SEM.

Resin removal – FAA-preserved specimens were embedded in Spurr's resin (Spurr 1969), sectioned at 1 µm thickness and heat-fixed to a circular glass coverslip. The coverslips with their specimens were passed through a series of chemicals designed to dissolve the resin leaving behind the specimen attached to the coverslip (Hogan & Smith 1982). Such specimens were sputter-coated with gold and viewed with the scanning electron microscope.

AFM

Herbarium samples – Air-dried wood samples were taken from various herbarium specimens (Table 1). Stem segments of 3 to 5 mm in length were split exposing the wood in radial longitudinal section. The samples were attached to AFM specimen metal disks (15 mm, Ted Pella, Inc.) using fingernail polish.

Specimens were imaged using a Veeco Dimension 3100 Scanning Probe Microscope as in a previous study (Dute & Elder 2011) and a Veeco NanoScope 3D. Images were captured at 512 × 512 resolution using TAP 150 tips, amplitude set point being approximately 1.8 V. Nanoscope 5.3lrl was used to save height, amplitude and phase images.

FAA samples – Chemically preserved and HMDS (solvent) dried specimens were mounted on AFM disks using fingernail polish and observed as above using AFM.

TEM

Herbarium samples – Air-dried, herbarium samples (Table 1) were processed for TEM using the technique of Dute *et al*. (1992). Briefly, small tissue cubes were immersed in three changes of acetone for approximately 1 h apiece. Specimens then were placed into 50 : 50 acetone : propylene oxide followed by 3 changes of propylene oxide (approximately 30 min. apiece). Spurr's plastic resin (Spurr 1969) was used for embedding. One-third resin in propylene oxide was followed by two-thirds resin, and pure resin each at 2-h intervals. Fresh resin was added, and specimens were placed in a vacuum for 1 h. The vacuum was released and the specimens left in resin at room temperature overnight. After another 8 hours in fresh resin, embedding occurred. Semithin sections were cut at Ulm University with a glass knife using an ultramicrotome (Ultracut E, Reichert-Jung, Austria), heat-fixed to a microscope slide, stained with 0.5 % toluidine blue in 0.1 phosphate buffer, and mounted in DPX (Agar Scientific, Stansted, UK). Ultra-thin sections (c. 90 nm) were cut using a diamond knife, attached to 300 mesh copper grids (Agar Scientific, Stansted, UK), and stained manually with lead citrate. Observations were carried out using a Zeiss EM 900 microscope (Carl Zeiss AG, Germany) at 80 kV accelerating voltage.

FAA samples – Chemically preserved specimens were dehydrated and embedded in Spurr's resin. Silver to light gold sections (approximately 800–900 nm thickness)

were cut at Auburn University using a diamond knife, mounted on copper grids and stained. After some trial and error, a 2-minute stain with lead citrate was found to be suitable. Stained sections were viewed with a Zeiss EM 10CR using 60 kV accelerating voltage.

RESULTS

General

Torus-bearing pits of *Ephedra* wood are circular (Fig. 1). The tori are also circular and are centrally located on the pit membrane.

TBO stained tori usually are pink to purple in contrast to the blue-green pit borders (Fig. 1). Tori stain poorly after brief (2 minutes) immersion in 1% $KMnO_4$ (Fig. 2).

SEM

SEM allows observations of entire pit membranes at a somewhat lesser resolution than either AFM or TEM. SEM observations of air-dried herbarium material show both non-aspirated and aspirated pit membranes (Fig. 3 vs. 4), the latter being in the majority. Distinct, radial microfibrils are visible under both circumstances. In membranes showing minimal damage, radial fibrils appear thickened and result from merger of microfibrils emanating from the torus (Fig. 5). Similar images of these composite, radial microfibrils were obtained from preserved specimens air-dried from HMDS (Fig. 6). In margo regions thought to exhibit little damage, the microfibril pattern can be quite complex with thick radial microfibrils connected by thinner fibrils (Fig. 5).

Unfortunately, pit membranes viewed with SEM frequently suffered damage induced by the heat of the electron beam. Figure 7 shows two adjacent pits in chemically dried material with different margo morphologies due to beam-induced damage. Higher accelerating voltages (*e.g.* 25 kV) were found to produce less damage. SEM of deplasticized sections of wood one to three μm thick was undertaken in an effort to image undamaged pit membranes. This effort proved unsuccessful.

The torus as seen with SEM is circular with a relatively undifferentiated surface. Only at high magnifications in HMDS-dried material is slight granulation encountered (Fig. 6). Plasmodesmatal channels are not evident (Fig. 5 & 6).

AFM of air-dried material

In air-dried wood, the pit membranes are aspirated (Fig. 8). At low magnification the torus surface is generally featureless with occasional, obscure microfibrils (Fig. 9). Sometimes a slightly roughened surface is encountered (Fig. 8).

Irregular regions of a non-microfibrillar material (*a la* Pesacreta *et al.* 2005) exist on surfaces of both torus and margo of air-dried pit membranes (Fig. 10). Amplitude images of the torus depict the material as a thin layer that is frequently interrupted, thus exposing the subtending surface. Phase images depict the material as black (Fig. 11). In the margo this non-microfibrillar material is localized where adjacent microfibrils touch one another (Fig. 11).

A distinct component of radial microfibrils is present in the margo of aspirated pit membranes (Fig. 8). Microfibrils with orientations other than radial exist in the margo

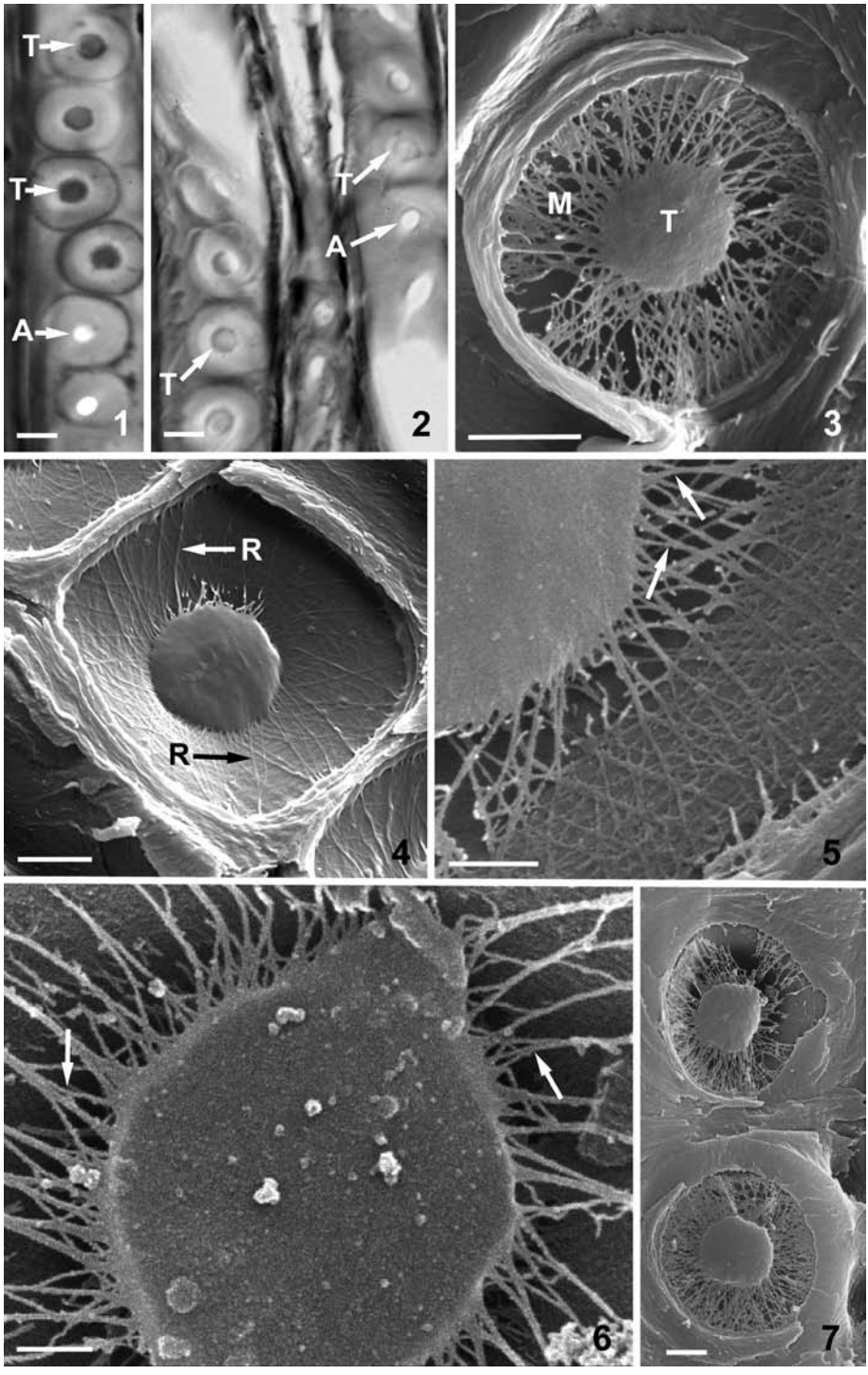
T
T
A
1
T
A
T
2
M
T
3
R
R
4
5
6
7

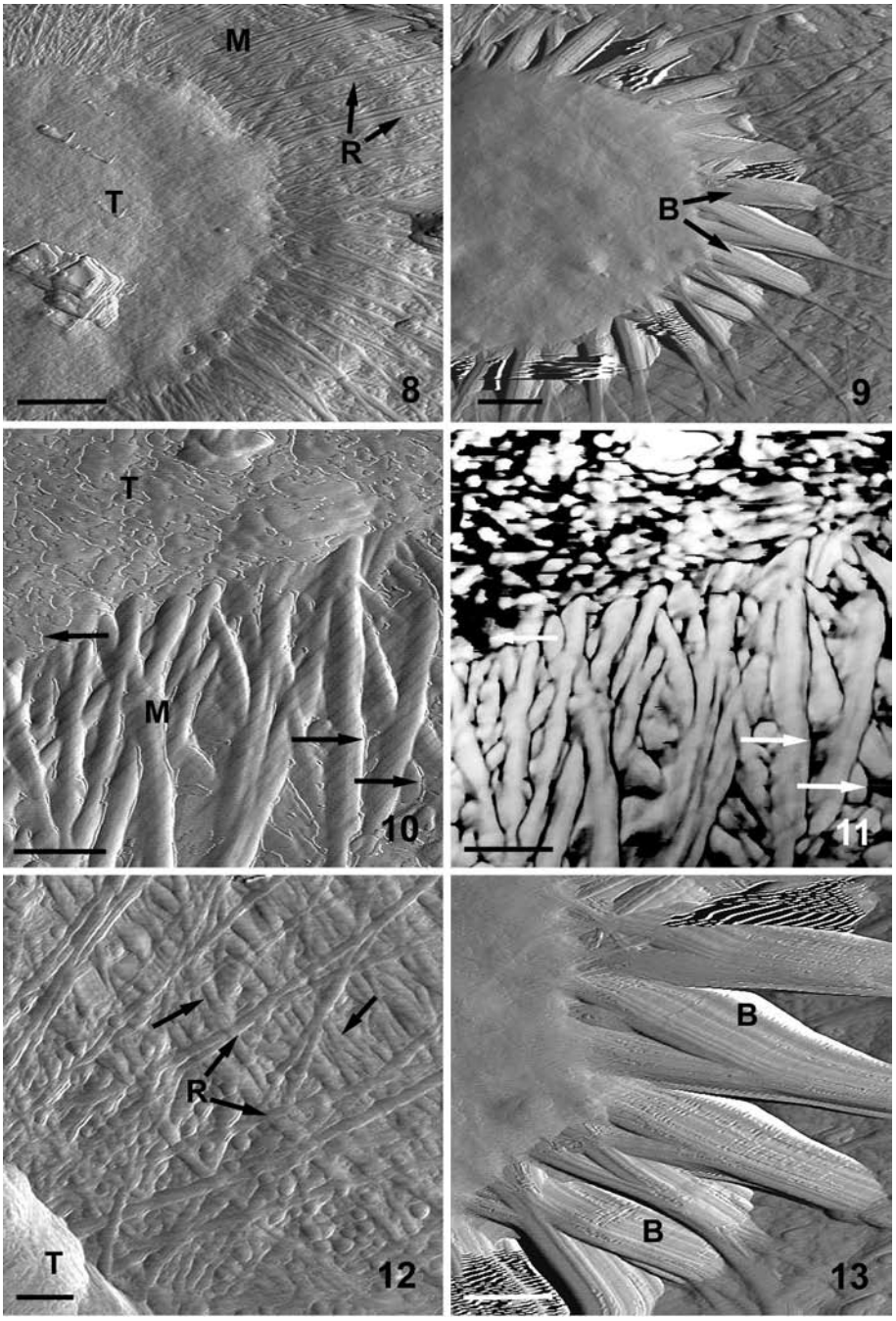

← Fig. 1–7 and ↑ Fig. 8–13: for legends, see page 224.

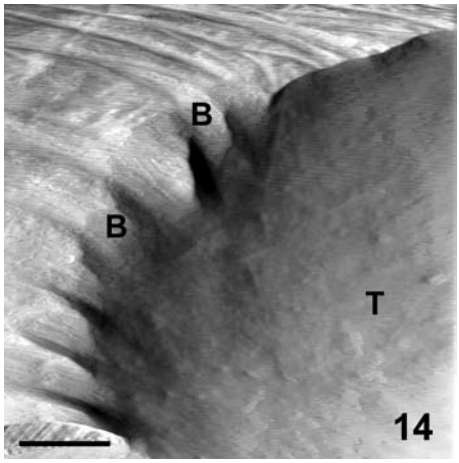

Fig. 14. AFM of aspirated pit membrane with buttresses and torus partially sunken into the aperture. – Scale bar = 400 nm.

(Fig. 12). Their precise relation to the overall structure of the margo is uncertain but appear to be largely at right angles to the radial fibrils.

Air-dried membranes of all species investigated have what can best be described as "buttresses" (Fig. 9) emerging from the torus in addition to the regular radial fibrils. The frequency of these buttresses varies from torus to torus. Detailed observations of the buttresses where they emerge from the torus show their composite nature (Fig. 13). Each buttress may well represent large, well-organized fascicles of microfibrils in

---

Abbreviations used in the figures in this study: A = aperture; AN = annulus; B = buttress; M = margo; PB = pit border; R = radially oriented microfibrils in the margo; T = torus. — Fig. 1–2, 6, 8, 10–12, 15–20, 22–27, 29 represent *Ephedra trifurca*; Fig. 3–5, 9, 13 represent *E. fasciculata*; Fig. 7, 21, 28 represent *E. torreyana*; Fig. 14 represents *E. viridis*.

←←

Fig. 1–7. LM and SEM of *Ephedra* pit membranes. – 1: LM of *E.* wood stained with toluidine blue O. – 2: LM of *E.* wood stained with potassium permanganate. – 3: Non-aspirated pit membrane. – 4: Aspirated pit membrane. Note distinct radial microfibrils (labeled arrows). – 5: Detail of partially aspirated pit membrane. Arrows indicate merger of radial microfibrils. – 6: Pit membrane dried from HMDS. Merger of radial microfibrils (arrows) and granulated torus surface are evident. – 7: Adjacent HMDS-dried pit membranes. – Scale bars = 5 μm for Fig. 1 & 2; 2 μm for Fig. 3, 4 & 7; 1 μm for Fig. 5; 500 nm for Fig. 6.

←

Fig. 8–13. AFM of air-dried herbarium specimens. – 8: Margo with distinct radial microfibrils. – 9: Pit membrane with buttresses. – 10: Torus and margo showing non-microfibrillar material (arrows) in amplitude image. – 11: Same as Fig. 10 but seen as phase image. Non-microfibrillar material (arrows) appears black. – 12: Detail of microfibril orientation in margo. Some microfibrils having an orientation other than radial are indicated by unlabeled arrows, whereas labeled arrows denote radial microfibrils. – 13: Detail of buttresses. – Scale bars = 1 μm for Fig. 8, 9; 200 nm for Fig. 10, 11; 250 nm for Fig. 12; 500 nm for Fig. 13.

close, parallel array from which a narrower, radial microfibril (or a small number of microfibrils) emerges (Fig. 9). Close inspection of images indicates that the individuality of the microfibrils within the buttresses can be lost (Fig. 13).

In aspirated pit membranes, buttresses give the impression of not allowing the torus to seal tightly against the pit border (Fig. 9). However, one instance was observed where the aperture extended beyond the edge of the torus, and in that case, the buttresses extended into the aperture cavity (Fig. 14).

AFM of chemically dried material

AFM observations of chemically dried pit membranes were restricted to wood specimens of *E. trifurca*. Mature pit margoes show areas of clustered microfibrils (fascicles) although the fascicles are not as pronounced as the buttresses in air-dried material (Fig. 15). Adhesion of microfibrils emerging from the torus is clearly observed in amplitude (Fig. 15), height (Fig. 16) and phase mode images. Detailed views of the margo show openings of different diameters among the microfibrils (Fig. 17).

The torus of chemically dried pit membranes is finely granular (Fig. 15, 16, 18). Some tori contain irregular projections from the surface (Fig. 18). Even at high magnification there is no concrete evidence of plasmodesmatal openings (Fig. 19).

Regions of non-microfibrillar material exist on the surfaces of some chemically dried pit membranes (Fig. 20) as they do on air-dried samples.

TEM & ontogeny of the margo in chemically dried material

Most TEM data were collected from FAA preserved samples of *E. torreyana* and *E. trifurca*. For these specimens, typical uranyl acetate/lead citrate staining of ultrathin sections led to overstaining of the mature torus, although the wall of the pit border exhibited proper stain density. Generally, optimal contrast of the torus was obtained through staining with lead citrate alone for two minutes.

→

Fig. 15–20. AFM of HMDS-dried specimens. – 15 & 16: Amplitude and height images of same area of pit membrane. Note the granular nature of the torus surface. Clustering of microfibrils is denoted at arrows. – 17: Detail of microfibrillar arrangement in margo. Openings of various sizes are apparent among the microfibrils (asterisks). – 18: Torus surface is granular with additional irregular projections (unlabeled arrows). – 19: Detail of torus surface. No plasmodesmatal openings are evident. – 20: Detail of margo with arrows indicating non-microfibrillar material. – Scale bars = 250 nm for Fig. 15, 16, 17; 500 nm for Fig. 18; 100 nm for Fig. 19, 20.

→ →

Fig. 21–26. TEM of pit membrane. – 21: Torus traversed by faint channels (asterisks). Extended membrane material (arrows) on torus surface is aligned with the channels. – 22: Plasmodesmatal branches (arrows) in torus. – 23: Complex, branched plasmodesmata at torus/margo juncture of an immature pit membrane. The juncture is marked by arrowheads; to the left is torus, to the right is margo. Cell at bottom is the younger and still contains cytoplasm. A faint desmotubule (arrow) is apparent. – 24–26: Clearing of matrix material from margo. Unlabeled arrows indicate fascicles of microfibrils connecting torus to annulus. – Scale bars = 500 nm for Fig. 21, 26; 250 nm for Fig. 22–25.

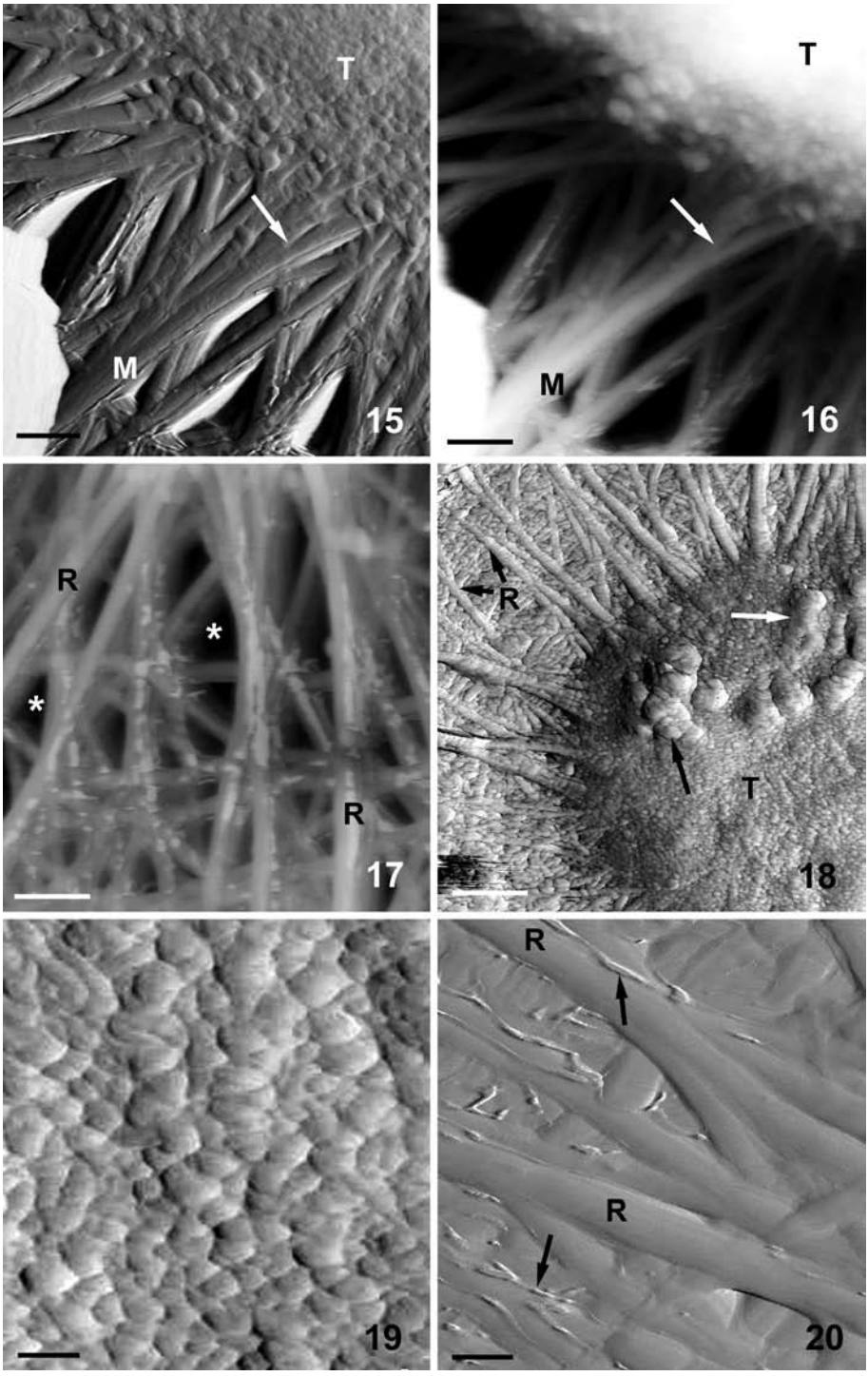
T
M
15
T
M
16
R
*
*
R
17
R
T
18
19
R
R
20

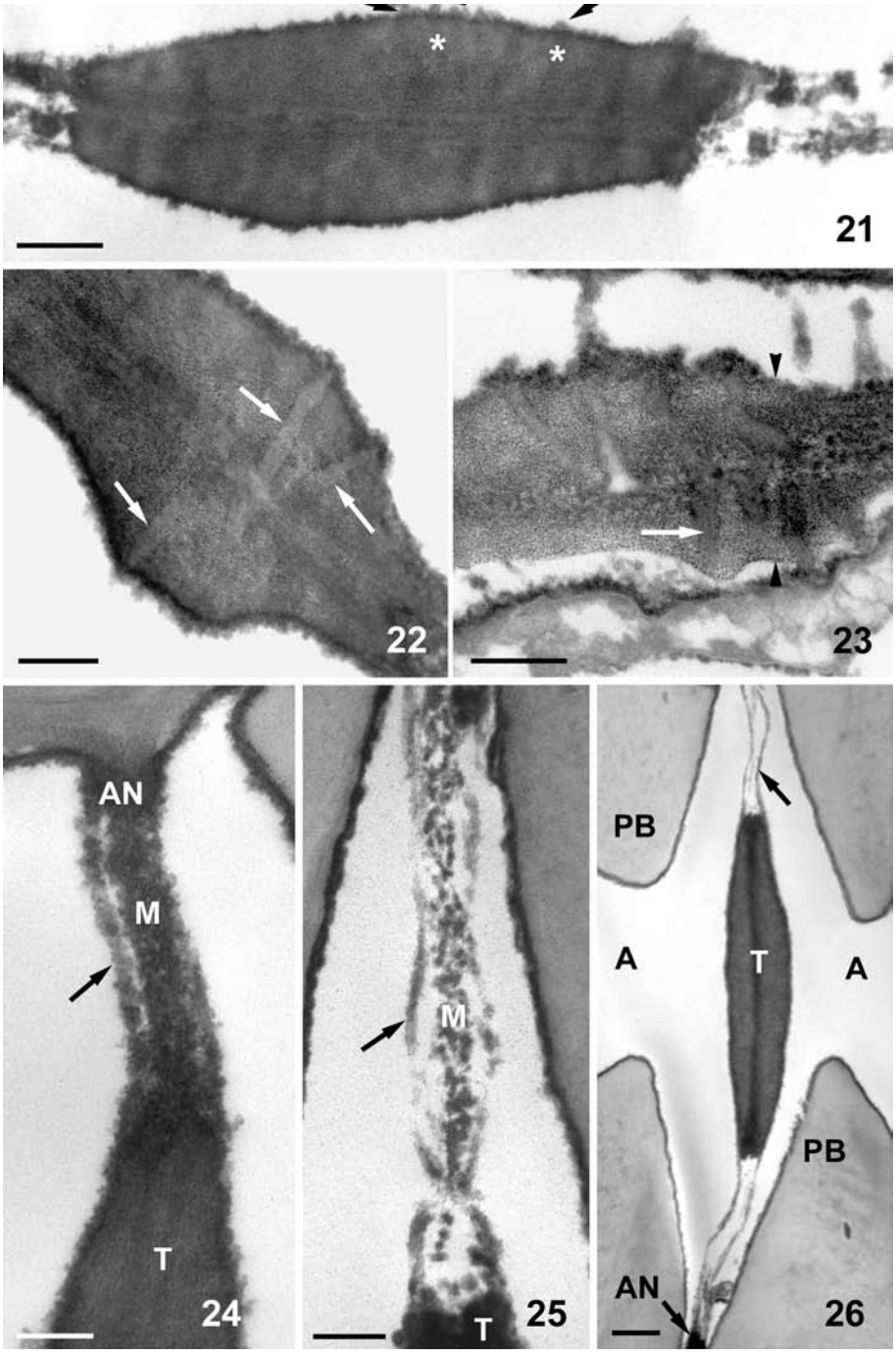

← Fig. 15–20 and ↑Fig. 21–26: for legends, see page 225.

Most tori in sectioned material had no clear plasmodesmata; however, some sections showed faint traces of possible channels. Figure 21 is a case in point. The cells have recently matured, and the torus surface is still covered by a remnant plasmalemma. Extension of membrane material from the surface of the torus into the cell lumen (Fig. 21, arrows) aligns with faint channels (see asterisks) in the torus. These channels are interpreted as plasmodesmata and the membrane extensions as either desmotubule traces or as extensions of the plasmalemma lining of the plasmodesmata. Distinct, complex, well-developed plasmodesmata occasionally were discovered in tori (Fig. 22) and in an immature pit membrane where torus and margo adjoin (Fig. 23). The plasmodesmata represent channels extending from median cavities in the middle lamella of the pit membrane to both surfaces. Such complex channels are referred to as secondary plasmodesmata. In some tori, channels took the form of half plasmodesmata passing from surface to middle lamella. TEM images of pit membranes from herbarium specimens also showed occasional plasmodesmata in the tori.

Transmission electron micrographs of pit margoes provide a partial developmental series of pit membrane maturation. Figure 23 is an immature pit membrane in which one adjoining tracheary element retains its cytoplasm, and the other does not. The poor quality of cytoplasmic preservation is probably due to the nature of the preservative. The left-hand portion of the membrane is the edge of the torus, whereas the right-hand portion is an immature margo. The latter shows increased stain uptake and granulation of wall components relative to the former. This stage is followed by increased electron density throughout the wall of the margo (Fig. 24). Even at this stage one or more strands of wall material connect the torus with the annulus (Fig. 24, arrow) and are thought to represent fascicles of microfibrils. As the granular matrix of the margo is lost, the remaining fascicles become more distinct (Fig. 25, 26). Note, with TEM the fascicle material appears restricted to the surfaces of the margo.

Confirmation of the TEM observations comes from pit membranes of FAA-fixed and HMDS-dried material seen with the AFM.

Figure 27 shows a margo during matrix removal. Clustering of radial microfibrils into fascicles is evident (arrows). Very fine microfibrils occur among the globular remains of the matrix material and correspond to narrower, non-radial microfibrils present in the mature margo (Fig. 17).

Disaggregation and removal of matrix material of the pit membrane occurred not only within the margo, but also to varying degrees in the middle region of the torus (identified as the middle lamella). In typical examples, matrix removal from the torus gives the latter the three-dimensional shape of a wheel whose rim is grooved. In other instances the amount of wall material removed from the middle lamella between the torus thickenings is more extensive and in extreme cases can lead to formation of two, separate torus pads (Fig. 28).

TEM of air-dried material

As might be expected, most pit membranes from herbarium specimens were aspirated. In such cases the margo is collapsed into a thin line, and the torus is so tightly appressed to the pit border that no line of demarcation is visible between the two

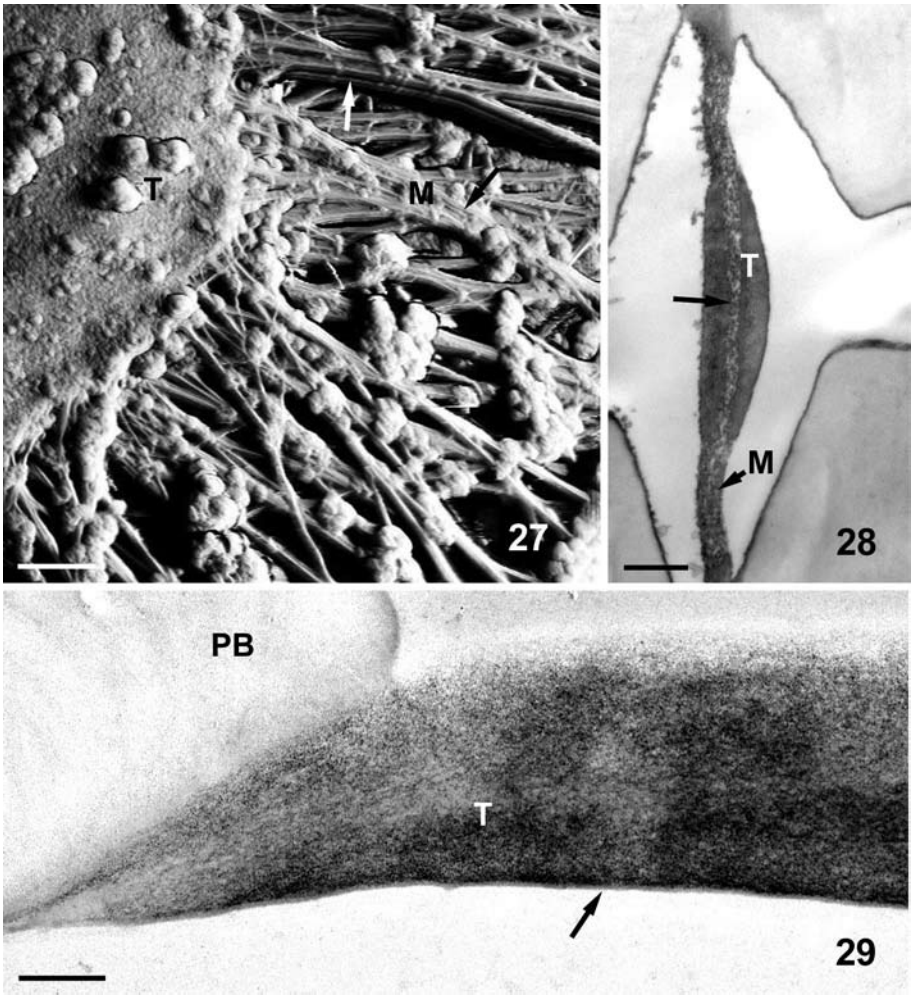

Fig. 27–29. – 27: AFM of matrix removal from margo. Arrows indicate fascicles. – 28: Example of pit membrane with matrix removed between the torus pads (unlabeled arrow). – 29: Portion of aspirated torus and pit border from herbarium specimen. Note the coating on the concave surface of the torus (arrow) and compare to the unaspirated torus surfaces in Fig. 22. – Scale bars = 500 nm for Fig. 27, 28; 250 nm for Fig. 29.

(Fig. 29). Also, a thin even layer often coats one surface of the torus, sometimes on the convex surface, sometimes on the concave (Fig. 29).

DISCUSSION

Intervascular pit membranes of *Ephedra* share features with pit membranes of both gymnosperms and angiosperms, but the shared resemblance is stronger with the former group. This premise is examined in the discussion.

AFM

This study has used different types of microscopy to investigate pit membrane structure and, to a certain extent, development in *Ephedra*. Advantages and disadvantages of light, scanning electron and transmission electron microscopy are well known, those of AFM less so because it is a newer type of imaging. In brief, a typical AFM "taps" the surface of a specimen with a fine pointed stylus. The resulting loss of amplitude of the cantilever arm to which the stylus is attached is used to manufacture an image (Dute & Elder 2011 and literature cited therein). AFM provides images superficially similar to SEM micrographs but with much superior resolution. Coating specimens is not needed and specimens are not exposed to a vacuum. Hydrated specimens can be imaged but were not in the present study. Different types of data sets can be obtained including height, amplitude and phase images (Pesacreta *et al*. 2005).

Plasmodesmata

Occasional tori of mature intervascular pit membranes of *Ephedra* possess distinct plasmodesmata. The branched nature of these cytoplasmic channels is reminiscent of similar structures found in mature tori of some conifers (*q.v*. discussion in Dute *et al*. 2008; Jansen *et al*. 2012) and in developing intervascular pit membranes of *Ginkgo* (Dute 1994). In developing tori of *Abies* (Dute *et al*. 2008) there are plasmalemma extensions from the sites of plasmodesmata into the cytoplasm similar to what is seen in *Ephedra*. Some gymnosperms, among them *Ginkgo* and *Metasequoia* (Dute 1994; Dute *et al*. 2008), have distinct plasmodesmata in torus and margo of immature intertracheary pit membranes only to have them disappear with maturation of the membrane and loss of matrix material. In other genera (such as *Abies*, Dute 2008) where the torus retains its matrix, plasmodesmata remain visible.

In contrast to the above, plasmodesmata in tori of angiosperm pit membranes are rare (Dute & Rushing 1988; Dute *et al*. 1990; Dute *et al*. 2010). Jansen *et al*. (2012) have shown a correlation between "punctured tori" of conifers and susceptibility to cavitation. Such being the case, one would expect *Ephedra*, a xerophyte, either to lack plasmodesmata in the torus altogether or to have the plasmodesmatal channels occluded. The drought resistant nature of this genus has been confirmed by xylem vulnerability curves (P. Bouche, pers. comm.).

The paucity of well-defined secondary plasmodesmata might represent the natural situation or might be due to changes in pit membrane structure that occur during ontogeny. Certainly, any plasmodesmata present in the immature margo would lose their integrity during maturation. The torus, as well, seems to undergo some changes during maturation. A developmental study of pit membranes of *Ephedra* is needed to assess accurately the frequency and appearance of plasmodesmata.

Plasmodesmata in tori of *Ephedra* were observed in this study using TEM, but not AFM, a type of microscopy comparable to TEM in resolving power (Hanley *et al*. 1992). This is noteworthy, as putative plasmodesmatal openings were observed on torus surfaces of *Pinus taeda* L. using AFM (Dute & Elder 2011). The situation in *Ephedra* points to the advantage of studying a system using multiple types of microscopy.

Most TEM observations were made on preserved material, and it could be argued that the fixative used in this study (FAA) did not provide optimal preservation and led to artifacts. FAA was chosen for its ease of use and long shelf-life under field conditions. We did not receive the type of cytoplasmic preservation typically attained *via* use of glutaraldehyde/osmium, yet, as seen in Figure 23, some unit membranes were preserved. The shapes of plasmodesmata obtained were typical of secondary plasmodesmata found in pit membranes of other gymnosperms (Dute 1994; Dute *et al*. 2008).

Coating material

Non-microfibrillar coating material, was found on surfaces of *Ephedra* pit membranes. Similar coating has been observed on intervascular pit membrane surfaces of *Sapium sebiferum* (L.) Roxb. by Pesacreta *et al*. (2005). One of the advantages of using AFM is that data can be presented in different forms (Pesacreta *et al*. 2005). Phase imaging, for example, indicates areas on specimens with different physical properties. Thus, phase images of black, non-microfibrillar material against lighter microfibrils indicate the former substance to be soft or viscous relative to the latter (Pesacreta *et al*. 2005). Comparing air-dried versus hydrated pit membranes using AFM, Pesacreta *et al*. noted that in the former, non-microfibrillar material coated the microfibrils, whereas in the latter, the non-microfibrillar material formed a distinct, separate layer from the microfibrils. The authors hypothesized that the non-microfibrillar layer regulated water passage across the membrane according to the mechanism of Zwieniecki *et al*. (2001). Lee *et al*. (2012), using AFM on hydrated pit membranes of *Nicotiana tabacum* L., observed changes in the surface upon addition of 50 mM KCl. Non-microfibrillar material of similar appearance to that in *Sapium* has also been observed with AFM in dried pit membranes of *Osmanthus armatus* Diels, *Cercocarpus montanus* Raf. and *Ulmus alata* Michx. (Dute & Elder 2011) as well as in pit membranes of other species (Jansen, pers. obs.). Regulation of water flux by coating material seems reasonable for pit membranes of angiosperms where passages among microfibrils are small, but we would consider it less tenable when associated with the relatively large openings in margoes of gymnosperms (Pittermann *et al*. 2005). A second hypothesis is suggested by Carlquist's work (2012) with *Ephedra nevadensis* S. Wats. in which he observed both aspirated and partially aspirated pit membranes. In the case of aspirated pit membranes, he discerned "merging" or "fusion" of margo threads to the surface of the pit border by hydrogels. Although the function of the coating is not clear, we would suggest that such fusion results from the action of the non-microfibrillar material seen with the AFM on the surface of the microfibrils and torus.

A major question concerns the chemistry of this non-microfibrillar coating. Recent experiments in the laboratory of one of the authors (S.J.) showed no protein accumulation in pit membranes (but see Harrak *et al*. 1999). Ca^{2+} has been reported in pit membranes by Opalka *et al*. (1998), and Ruel *et al*. (2012) reported limited amounts of amorphous cellulose in intervessel pit membranes of *Arabidopsis*. Pectin is typically associated with torus structure of conifers (Hafrén *et al*. 2000; literature cited in Coleman *et al*. 2004; Putoczki *et al*. 2008). The situation is further obscured by treatment effects. When comparing the torus surface of chemically preserved (Fig. 22) *versus*

air-dried herbarium material (Fig. 29) one detects the roughened and smooth surfaces, respectively. These observations correlated with AFM images of chemically fixed (Fig. 15) and air-dried (Fig. 9) torus surfaces. One possible explanation is that wound material, probably pectins (Fujino *et al*. 1983; Dute *et al*. 1992 and literature therein), is deposited on the torus surface during the drying process thus creating a smoother surface, or that the physical act of pit membrane aspiration rearranges the features of the torus surface.

Microfibril orientation

Radially oriented microfibrils are a distinct feature of the margo of pit membranes in conifers. Liese (1965), using the replica technique, observed radial microfibrils in margoes of the Pinaceae. Thick radial fibrils were first observed in immature pit membranes and were formed by combination of individual fibrils followed by reorientation of the resulting cables. In the immature membrane other microfibrils were attached in a tangential direction. In mature margoes the diameter of the radial strands exists as either individual microfibrils or as "fasciculated" ones that have joined during differentiation. Thickness of fasciculated microfibrils is increased during aspiration.

Fengel (1966) commented upon the bundling of microfibrils in the margo of *Picea abies* during "pit closure" (aspiration). Banks (1971), who studied various conifers, correlated change in appearance of radial fibrils during aspiration to restriction of the microfibrils' location from three dimensions to two. Bauch *et al*. (1972) confirmed the presence of radial fibrils in the margo of conifers as well as in *Ginkgo*. They also verified the presence of tori in pit membranes of two species of *Ephedra* and described a definite radial orientation to the margo microfibrils. Fengel (1972) noted increase in radial orientation and coalescence of microfibrils during pit aspiration in softwoods. Puritch & Johnson (1973) observed sapwood of fir that was freeze-etched from its normal conducting state. The margo consisted of "large radial strands with numerous crossbars." "The larger strands fanned out into smaller fibrils as they approached the torus or edge of the pit chamber." The consensus of this early work is that the margo of conifer and *Ginkgo* pits has a distinct radial component of microfibrils cross-linked by small diameter fibrils. Thickness of the radial fibers increases with aspiration. Associated with this microfibrillar pattern in the pit membrane is the presence of margo pores (measured in tenths of micrometers – Pittermann *et al*. 2005; Banks 1971; Dute 1994; Dute *et al*. 2008; Jansen *et al*. 2012).

An example of radial microfibrils associated with the developing pit membrane can be found in *Ginkgo biloba* (Dute 1994). TEM of ultrathin sections cut parallel to the surface of intertracheary pit membranes shows radial striations emanating from the torus. However, like the situation in the Pinaceae (Liese 1965), the radial components in *Ginkgo* become more distinct during aspiration.

The margo of *Ephedra* did not go unnoticed by investigators studying pit membranes *via* electron microscopy. Liese (1965) published a micrograph of a replica of an *E. campylopoda* C.A.Mey. pit membrane. He described the margo as having a "dense primary wall texture" although a radial microfibrillar component was clearly visible in the micrograph. Work of Bauch *et al*. (1972) was mentioned previously. Carlquist

(1992), using SEM, noted resemblance of margo strands in membranes of Old World *Ephedra* spp. to those in pit membranes of conifers. In a more detailed SEM study of *E. nevadensis*, Carlquist (2012) showed the different appearances of the margo, similar to what we have seen in the present study. We would explain this diversity as a result of damage due to processing and/or heat of the electron beam.

From our studies we would conclude that orientation of margo microfibrils in *Ephedra* is much as described by Liese (1965) for the Pinaceae. Radial microfibrils are distinct and often form fascicles. In aspirated pit membranes extreme examples of fasciculation, the so-called "buttresses" are formed. Precise arrangement of microfibrils within the buttresses remains uncertain. Fasciculated microfibrils appear to be restricted to both surfaces of non-aspirated pit membranes according to our TEM data. A similar positioning of radial microfibrils has been noted by Thomas (1970) for *Pinus*.

In contrast to the above-mentioned membranes, most intervascular pit membranes of angiosperms have randomly distributed microfibrils associated with micropores of nanometer-scale diameter (Pittermann *et al*. 2005; Jansen *et al*. 2009). An exception to this description is the torus-bearing intervascular pit membranes of angiosperms where there are various densities of microfibrils radiating from the torus and traversing the surface of the membrane (Wheeler 1983; Dute & Elder 2011). Nevertheless, these particular pit membranes also have randomly distributed, "tightly woven" microfibrils with micropores rather than the relatively large pores found in conifers, *Ginkgo* (Pittermann *et al*. 2005; Dute & Elder 2011) and *Ephedra* (this ms.).

Other pit features

Although developmental stages were not observed in the present study, the torus in *Ephedra* appears to consist of primary wall thickenings rather than distinct, secondary pads. This mode of construction is found in conifers (Dute *et al*. 2008 and literature therein) and in *Ginkgo* (Dute 1994), but in only some genera of torus-bearing angiosperms.

Preliminary evidence from this study indicates that tori of mature pit membranes of *Ephedra* are not lignified. This evidence distinguishes *Ephedra* from the angiosperms *Daphne* and *Osmanthus* (Coleman *et al*. 2004), but not from other gymnosperms (*q.v.* discussion in Jansen *et al*. 2012).

ACKNOWLEDGEMENTS

We wish to thank Drs. Aaron Rashotte and Christine Sundermann for use of their microscopes and Curtis J. Hansen for his assistance in identifying collected specimens of *Ephedra*. The Electron Microscopy Section of Ulm University is acknowledged for technical assistance with preparing TEM samples. This work was supported by the Alabama Agriculture Experiment Station and by an undergraduate Research Grant-In-Aid from the Department of Biological Sciences, Auburn University.

REFERENCES

Banks WB. 1971. Structure of the bordered pit membrane in certain softwoods as seen by scanning electron microscopy. J. Inst. Wood Sci. 5: 12–15.

Bauch J, Liese W & Schultze R. 1972. The morphological variability of the bordered pit membranes in gymnosperms. Wood Sci. Technol. 6: 165–184.
Carlquist S. 1992. Wood, bark, and pit anatomy of Old World species of *Ephedra* and summary for the genus. Aliso 13: 255–295.
Carlquist S. 1994. Wood and bark anatomy of *Gnetum gnemon* L. Bot. J. Linn. Soc. 116: 203–221.
Carlquist S. 1996. Wood, bark and stem anatomy of New World species of *Gnetum*. Bot. J. Linn. Soc. 120: 1–19.
Carlquist S. 2012. Wood anatomy of Gnetales in a functional, ecological, and evolutionary context. Aliso 30: 33–47.
Carlquist S & Gowans DA. 1995. Secondary growth and wood histology of *Welwitschia*. Bot. J. Linn. Soc. 118: 107–121.
Carlquist S & Robinson AA. 1995. Wood and bark anatomy of the African species of *Gnetum*. Bot. J. Linn. Soc. 118: 123–137.
Coleman CM, Prather BL, Valente MJ, Dute RR & Miller ME. 2004. Torus lignification in hardwoods. IAWA J. 25: 435–447.
Donaldson LA. 2002. Abnormal lignin distribution in wood from severely drought stressed hardwoods. IAWA J. 23: 161–178.
Dute RR. 1994. Pit membrane structure and development in *Ginkgo biloba*. IAWA J. 15: 75–90.
Dute RR & Elder T. 2011. Atomic force microscopy of torus-bearing pit membranes. IAWA J. 32: 415–430.
Dute R, Hagler L & Black B. 2008. Comparative development of intertracheary pit membranes in *Abies firma* and *Metasequoia glyptostroboides*. IAWA J. 29: 277–289.
Dute RR, Patel J & Jansen S. 2010. Torus-bearing pit membranes in *Cercocarpus*. IAWA J. 31: 53–66.
Dute RR & Rushing AE. 1988. Notes on torus development in the wood of *Osmanthus americanus* (L.) Benth. & Hook. *ex* Gray (Oleaceae). IAWA Bull. n.s. 9: 41–51.
Dute RR & Rushing AE. 1990. Torus structure and development in the woods of *Ulmus alata* Michx., *Celtis laevigata* Willd., and *Celtis occidentalis* L. IAWA Bull. n.s. 11: 71–73.
Dute RR, Rushing AE & Freeman JD. 1992. Survey of intervessel pit membrane structure in *Daphne* species. IAWA Bull. n.s. 13: 113–123.
Dute RR, Rushing AE & Perry JW. 1990. Torus structure and development in species of *Daphne*. IAWA Bull. n.s. 11: 401–412.
Dute RR, Zwack PJ, Craig E & Baccus SM. 2012. Torus presence and distribution in leaves of *Osmanthus armatus*. IAWA J. 33: 257–268.
Fengel D. 1966. Entwicklung und Ultrastruktur der Pinaceen-Hoftüpfel. Svensk Papp-Tidn. 69: 232–241.
Fengel D. 1972. Structure and function of the membrane in softwood bordered pits. Holzforschung 26: 1–9.
Friedman WE. 1990. Double fertilization in *Ephedra*, a nonflowering seed plant: its bearing on the origin of angiosperms. Science 247: 951–954.
Frohlich MW & Chase MW. 2007. After a dozen years of progress the origin of angiosperms is still a great mystery. Nature 450: 1184–1189.
Fujino DW, Reid MS & van der Molen GE. 1983. Identification of vascular blockages in rachids of cut Maidenhair (*Adiantum raddianum*) fronds. Sci. Hortic. (Neth.) 21: 381–388.
Hafrén J, Daniel F & Westermark A. 2000. The distribution of acidic and esterified pectin in cambium, developing xylem and mature xylem of *Pinus sylvestris*. IAWA J. 21: 157–168.
Hanley SJ, Giasson J, Revol J-F & Gray DG. 1992. Atomic force microscopy of cellulose microfibrils: comparison with transmission electron microscopy. Polymer 33: 4639–4642.

Harrak H, Camberland H, Plante M, Bellemare G, Lafontaine JG & Tabaeizadeh Z. 1999. A proline-, threonine-, and glycine-rich protein down-regulated by drought is localized in the cell wall of xylem elements. Pl. Physiol. 121: 557–564.

Hogan DL & Smith GH. 1982. Unconventional application of standard light and electron immunocytochemical analysis to aldehyde-fixed, araldite-embedded tissues. J. Histochem. Cytochem. 30: 1301–1306.

Jansen S, Choat B & Pletsers A. 2009. Morphological variation of intervessel pit membranes and implications to xylem function in angiosperms. Amer. J. Bot. 96: 409–419.

Jansen S, Lamy J-B, Burlett R, Cochard H, Gasson P & Delzon S. 2012. Plasmodesmatal pores in the torus of bordered pit membranes affect cavitation resistance of conifer xylem. Plant, Cell and Environment 35: 1109–1120.

Johansen DA. 1940. Plant microtechnique. McGraw-Hill Book Company, Inc., New York.

Joshi VC & Khan I. 2005. Macroscopic and microscopic authentication of Chinese and North American species of *Ephedra*. J. of AOAC International 88: 707–713.

Lee J, Holbrook NM & Zwieniecki MA. 2012. Ion induced changes in the structure of bordered pit membranes. Frontiers in Plant Science 3: 1–4.

Liese W. 1965. The fine structure of bordered pits in softwoods. In: Côté WA (ed.), Cellular ultrastructure of woody plants: 271–290. Syracuse University Press.

Nation JL. 1983. A new method using hexamethyldisilazane for preparation of soft insect tissues for scanning electron microscopy. Stain Technol. 58: 347–351.

Opalka N, Brugidou C, Bonneau C, Nicole M, Beachy RN, Yeager M & Fauquet C. 1998. Movement of rice yellow mottle virus between xylem cells through pit membranes. Proc. Natl. Acad. Sci. USA 95: 3323–3328.

Pesacreta TL, Groom LH & Rials TG. 2005. Atomic force microscopy of the intervessel pit membrane in the stem of *Sapium sebiferum* (Euphorbiaceae). IAWA J. 26: 397–426.

Pittermann J, Sperry JS, Hacke UG, Wheeler JK & Sikkema EH. 2005. Torus-margo pits help conifers compete with angiosperms. Science 310: 1924.

Price RA. 1996. Systematics of the Gnetales: a review of morphological and molecular evidence. Int. J. Plant Sci. 157 (6 Suppl.): S40–S49.

Puritch GS & Johnson RPC. 1973. The structure of freeze-etched bordered-pit membranes of *Abies grandis*. Wood Sci. Technol. 7: 256–260.

Putoczki TL, Gerrard, JA, Butterfield BG & Jackson SL. 2008. The distribution of un-esterified and methyl-esterified pectic polysaccharides in *Pinus radiata*. IAWA J. 29: 115–127.

Ruel K, Nishiyama Y & Joseleau J-P. 2012. Crystalline and amorphous cellulose in the secondary walls of *Arabidopsis*. Plant Science 193-194: 48–61.

Ruzin SE. 1999. Plant microtechnique and microscopy. Oxford University Press, New York.

Spurr AR. 1969. A low viscosity epoxy resin embedding medium for electron microscopy. J. Ultrastruct. Res. 26: 31–45.

Thomas, RJ. 1970. Origin of bordered pit margo microfibrils. Wood & Fiber 2: 285–288.

Thompson WP. 1912. The anatomy and relationships of the Gnetales. I. The genus *Ephedra*. Ann. Bot. 26: 1077–1104.

Thompson WP. 1918. Independent evolution of vessels in Gnetales and angiosperms. Bot. Gaz. 65: 83–90.

Wheeler EA. 1983. Intervascular pit membranes in *Ulmus* and *Celtis* native to the United States. IAWA Bull. n.s. 4: 79–88.

Zwieniecki MA, Melcher PJ & Holbrook NM. 2001. Hydrogel control of hydraulic resistance in plants. Science 291: 1059–1062.

Accepted: 18 February 2014